

Alma Mater Studiorum Università di Bologna
Archivio istituzionale della ricerca

A novel adaptive-gain technique for high-order sliding-mode observers with application to electro-hydraulic systems

This is the final peer-reviewed author's accepted manuscript (postprint) of the following publication:

Published Version:

Palli G., Strano S., Terzo M. (2020). A novel adaptive-gain technique for high-order sliding-mode observers with application to electro-hydraulic systems. MECHANICAL SYSTEMS AND SIGNAL PROCESSING, 144, 1-11 [10.1016/j.ymssp.2020.106875].

Availability:

This version is available at: <https://hdl.handle.net/11585/756890> since: 2020-04-27

Published:

DOI: <http://doi.org/10.1016/j.ymssp.2020.106875>

Terms of use:

Some rights reserved. The terms and conditions for the reuse of this version of the manuscript are specified in the publishing policy. For all terms of use and more information see the publisher's website.

This item was downloaded from IRIS Università di Bologna (<https://cris.unibo.it/>).
When citing, please refer to the published version.

(Article begins on next page)

This is the final peer-reviewed accepted manuscript of:

Gianluca Palli, Salvatore Strano, Mario Terzo, A novel adaptive-gain technique for high-order sliding-mode observers with application to electro-hydraulic systems, Mechanical Systems and Signal Processing, Volume 144, 2020, 106875, ISSN 0888-3270.

The final published version is available online at:

<https://doi.org/10.1016/j.ymssp.2020.106875>

Terms of use:

Some rights reserved. The terms and conditions for the reuse of this version of the manuscript are specified in the publishing policy. For all terms of use and more information see the publisher's website.

This item was downloaded from IRIS Università di Bologna (<https://cris.unibo.it/>)

When citing, please refer to the published version.

A Novel Adaptive-Gain Technique for High-Order Sliding-Mode Observers with Application to Electro-Hydraulic Systems

Gianluca Palli^{*,a}, Salvatore Strano^b, Mario Terzo^b

^a*DEI - Università di Bologna, Viale Risorgimento 2, 40132 Bologna, Italy*

^b*DII - Università degli Studi di Napoli Federico II, via Claudio 21, 80125 Napoli, Italy*

Abstract

In this paper, a novel technique for adaptive gain selection in high-order sliding mode observers to estimate the state and the disturbance acting on a hydraulic actuators is designed and tested. The proposed gain adaptation technique is based on the evaluation of the absolute value of the errors computed between the real measurements available on the system and their estimation provided by the observer.

Experimental results are reported to validate the effectiveness of the proposed technique in a real context. The experiment are conducted in two different conditions, i.e. without external load and with an unknown visco-elastic seismic isolator attached to the hydraulic actuator.

The proposed gain-adaptation method is also compared with the case of manually-tuned gains and a classic gain adaptation technique reported in literature, in which the gain adaptation is based on fixed variation rates. The proposed method provides performance comparable or superior to both manual and classic adaptive gain selection. Moreover, with respect to classic techniques, the proposed one has the advantage of improving the convergence rate in case of large estimation errors and limiting the growing of observer gains in case of noisy measurements.

Key words: Hydraulic actuators, high-order observers, adaptive gains, nonlinear systems.

1. Introduction

Electro hydraulic actuators (EHAs) are widely adopted in modern industries. Typical usage concerns heavy duty excavation, positioning systems [1] and vibration control [2, 3]. Within this contest, observers for state estimation based on mathematical models of EHAs are valid solutions for fault detection and diagnostics [4, 5, 6]. At the same time, state observers are a valid alternative

^{*}Corresponding author

Email address: gianluca.palli@unibo.it (Gianluca Palli)

to the installation of sensors to give feedback to the control laws in case of prohibitive costs or harsh environments [7]. The design of state observers should take into account the nonlinearities of hydraulic actuators such as frictions, pressure-flow rate relationship and dead-zone frequently encountered in many actuators of industrial control systems, especially those containing some very common components, such as hydraulic or pneumatic valves. Dead-zone nonlinearity often occurs in closed centre valves when the land width is greater than the port width at neutral spool position [8]. The presence of dead-zone, together with other nonlinearities of EHAs, makes the design of the state observers a challenging problem. Several approaches are proposed in literature. These methods include linear approaches, linearized model based techniques [9] and observers based on nonlinear models [10, 11]. Extended Kalman filter (EKF) is adopted to detect the fault in hydraulic actuators [12] by means of the state estimation. The approach is based on the local linearization of the nonlinear system and allows to closely track the state trajectories if compared with the linear approach of the Kalman filter [13]. Halder [14] showed a procedure to detect and isolate the sensor fault of an EHA system using conventional EKF. An unscented Kalman Filter based approach is presented in [15]. In [16] an active disturbance rejection adaptive control scheme based on full state feedback for motion control of hydraulic servo systems subjected to both parametric uncertainties and uncertain nonlinearities is proposed. In [17] an extended state observer and a nonlinear robust controller are synthesized via the backstepping method to manage a hydraulic system with mismatched modelling uncertainties. In [18], a nonlinear approach based on the State-Dependent-Riccati-Equation (SDRE) is proposed together with experimental validation. The high degree of parametric uncertainty that characterizes hydraulic actuators exhorts the researchers to follow robust approaches for the state estimation [19, 20]. In [21], the authors proposed a method based on robust filter structure, to compensate the effect of the unmodelled dynamics, combined with on-line parameter adaptation, to account for the parametric uncertainty. In [22] an adaptive disturbance compensation strategy based on sliding mode extended state observer is proposed for permanent magnet synchronous motors driven by voltage source inverters, while in [23] the authors reported an optimal fuzzy disturbance observer-enhanced sliding mode controller for magneto-rheological damper semi-active train-car suspensions. An extended state observer based on robust adaptive dynamic sliding mode tracking control for an automobile engine electronic throttle system is presented in [24]. In [25], an adaptive sliding mode observer (SMO) is proposed for the estimates of velocity and parameters of an electro-hydraulic system. Even if SMO is a valid tool to manage uncertainties, it is well known that the undesirable chattering phenomenon will degrade

the estimation performance and then a low pass filter is required for the reconstruction of the uncertainties. To overcome this limit, higher order sliding mode observers (HSMOs) are generally adopted due to their better sliding accuracy [26]. The use of HSMOs for state and unknown input estimation in uncertain nonlinear systems are discussed in [27, 28, 29, 30]. In [31], the authors present a HSMO for the estimation of road adhesion coefficient under various surface conditions. In a previous paper [32], the authors presented a comparison between a SMO, a HSMO and an EKF for state estimation in hydraulic actuators in presence of several nonlinearities. The results highlighted that HSMO presents in general a more reliable behaviour. Previous methods for gain adaptation in HSMO are applied in [33, 34] to fuel cells and power converters, while in [35] the application of adaptive gain HSMO to synchronous motors state identification is presented.

In this paper, a novel technique for the design of the Adaptive-gain HSMO (called A+HSMO to distinguish it from classic adaptation methods) gains is proposed and compared to a technique proposed in literature [34, 35] (we will refer to this technique as AHSMO in the following), where the adaptation is performed at a constant rate when the absolute estimation error is larger than a given threshold. The proposed A+HSMO is based on the fully nonlinear nominal EHA model, including also hard nonlinearities such as dead-zone of the control valve and friction on the piston, and it is used to estimate the full EHA state. Differently from previous techniques, in the A+HSMO the gain adaptation rate is proportional to the error absolute value, in such a way to speed up the convergence in case of large errors and to avoid the gains to grow unnecessarily in case of small errors. Stability proof is provided for the proposed technique, highlighting that how the proposed approach preserves the general properties of finite-time convergence of HSMO. Experiments are performed on an EHA shown in Fig. 1 in two different working conditions, i.e. without any load and with a visco-elastic load, to validate the A+HSMO and to compare its performances with manually tuned HSMO and AHSMO.

The paper is organized as follows: a fifth order nonlinear model is derived in Section 2 taking into account dead-zone, frictions and the nonlinear pressure-flow rate relationship; Section 3 focuses on HSMO design and introduces adaptive-gain strategies and stability analysis for the A+HSMO. The experimental results and their comparison are presented in Sec. 4, while conclusions are drawn in Sec. 5.

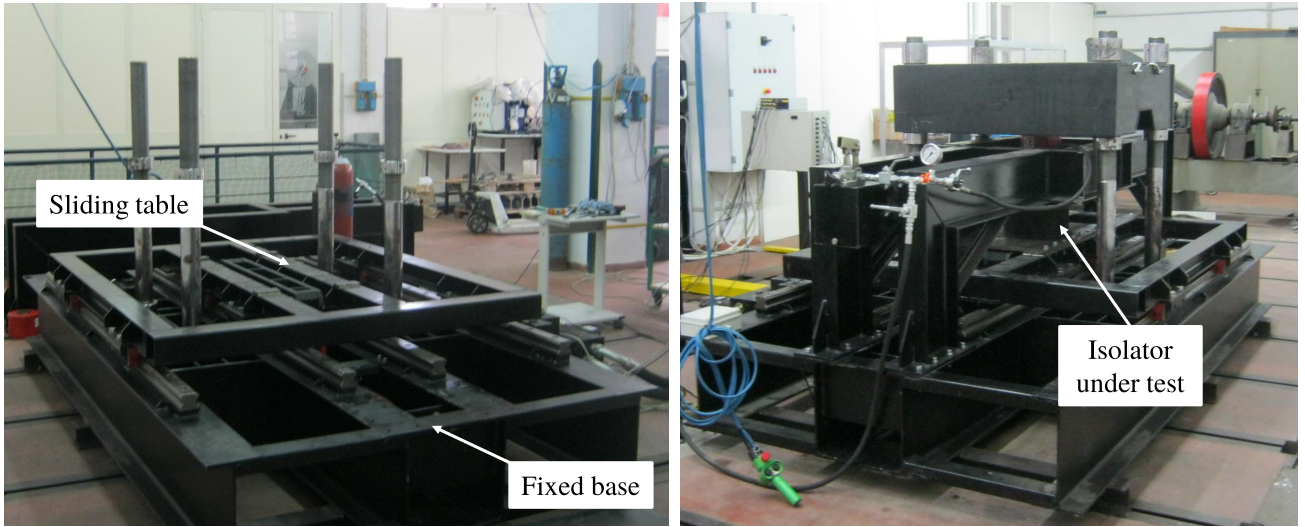


Figure 1: The seismic isolator used during the experiments.

2. System Dynamics

The EHA under consideration is part of a test rig shown in Fig. 1 and presented in [32], adopted for the experimental characterization of anti-vibration systems. The EHA mainly consists of a double-rod hydraulic cylinder linked to a mass (the sliding table) that moves on a linear guide. The flow distribution is controlled by a proportional valve and loads act on the moving mass. A scheme of the system is reported in Fig. 2. For the derivation of the mathematical model, some assumptions are made: the tank pressure P_T is equal to zero, the fluid properties are not dependent on the temperature, the piston areas and the chamber volumes are equal on both piston sides, the internal and external fluid leakages are negligible. The time dependence of the variables is omitted in the equations for brevity.

As derived in [32], the mathematical model of EHA is:

$$\begin{cases} \ddot{y} = -\frac{b}{m}\dot{y} - \frac{F_f(\dot{y})}{m} + \frac{A_p P_L}{m} \\ \dot{P}_L = -\frac{2\beta A_p}{V_0}\dot{y} + \frac{2\beta \Psi(v_e)\sqrt{P_s - |P_L|}}{V_0} \\ \ddot{v}_e = -\omega_{nv}^2 v_e - 2\epsilon_v \omega_{nv} \dot{v}_e + \omega_{nv}^2 (k_e u + v_{e0}) \end{cases} \quad (1)$$

where m is the mass of the load, b is the viscous friction coefficient, $F_f(\dot{y})$ is the friction force, A_p is the piston area, $P_L(t) = P_A(t) - P_B(t)$ is the load pressure, $P_A(t)$ and $P_B(t)$ are the pressures inside the two cylinder chambers, V_0 is the volume of each chamber for the piston centered position, β is the effective Bulk modulus, $v_e(t)$ is the spool valve displacement signal, ω_{nv} and ϵ_v are the natural frequency and the damping ratio of the valve respectively, v_{e0} is the spool position bias, k_e is the

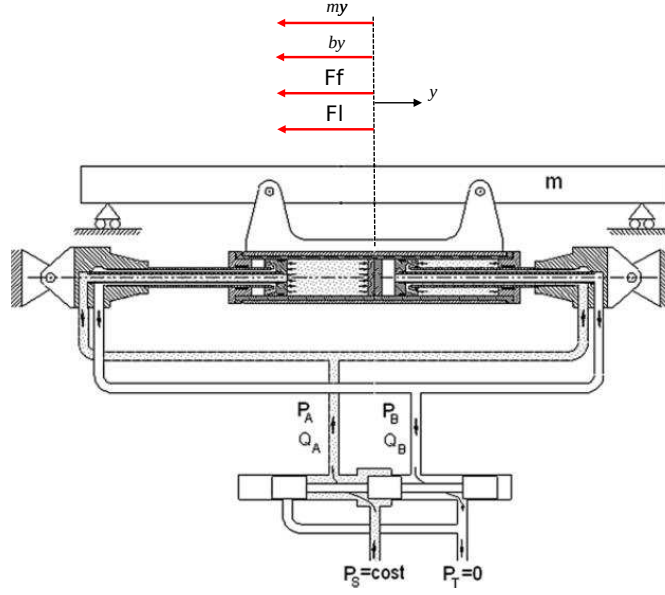


Figure 2: Schematic diagram of the hydraulic actuation system.

input gain and $u(t)$ is the valve command. See Tab. 1 for the description and the values of the system parameters.

In (1), the first line described the piston rod dynamics, including any other model part connected to it, the second represents the load pressure dynamics according to [36], while the third line resembles the proportional valve dynamics [37].

The function $\Psi(v_e)$ represents the valve nonlinear gain, which is supposed to be unknown. For the sake of simplicity and since the designed observer will cope with model uncertainties, a simple linear valve model is assumed in the system dynamics, i.e. $\tilde{\Psi}(v_e) = k_q v_e$.

Therefore, assuming as state vector $x(t) = [y(t) \ \dot{y}(t) \ P_L(t) \ v_e(t) \ \dot{v}_e(t)]^T$, the system (1) is nonlinear in the state and affine in the input $u(t)$. It follows that it can be rewritten as:

$$\dot{x}(t) = f(x(t)) + g(x(t)) u(t) + \varphi(x(t), t) \quad (2)$$

$$z(t) = h(x(t)) \quad (3)$$

with the assumptions

$$f(x(t)) = \begin{bmatrix} \dot{y} \\ -\frac{b}{m}\dot{y} + \frac{A_p P_L}{m} \\ -\frac{2\beta A_p}{V_0}\dot{y} + \frac{2\beta k_q v_e \sqrt{P_s - |P_L|}}{V_0} \\ \dot{v}_e \\ -\omega_{nv}^2 v_e - 2\epsilon_v \omega_{nv} \dot{v}_e \end{bmatrix} \quad (4)$$

$$g(x(t)) = \begin{bmatrix} 0 \\ 0 \\ 0 \\ 0 \\ \omega_{nv}^2 k_e \end{bmatrix}, \quad h(x(t)) = \begin{bmatrix} y \\ P_L \\ v_e \end{bmatrix} \quad (5)$$

$$\varphi(x(t), t) = \begin{bmatrix} 0 \\ -\frac{F_f(\dot{y})}{m} + \eta_y(t) \\ \frac{2\beta(\Psi(v_e) - k_q v_e) \sqrt{P_s - |P_L|}}{V_0} + \eta_{P_L}(t) \\ 0 \\ \omega_{nv}^2 v_{e0} + \eta_{v_e}(t) \end{bmatrix} \quad (6)$$

where $z(t)$ is the output vector, $f(x(t), u(t))$, $\varphi(x(t), t)$ and $h(x(t))$ are the state dynamics, the disturbance and the output non-linear functions respectively, $g(x(t))$ is the input function, $u(t)$ is the system input, k_q is the nominal valve constant, and the function $\eta(t) = [\eta_y(t), \eta_{P_L}(t), \eta_{v_e}(t)]^T$ includes unmodelled loads, dynamics and parameter uncertainties.

3. HSMO Design

The full procedure for the HSMO design is reported in [32], here the results are briefly summarized for clarity.

First, it can be easily verified that the sum of the output relative degrees is equal to 5, i.e. the dimension of whole state space, meaning that there is no hidden dynamics in the system given the output vector $z(t)$. It follows that, by indicating with the $\hat{\cdot}$ the estimated variables, the system (2) can be rewritten in block-wise Brunovsky canonical form as:

$$\dot{\hat{x}} = \Lambda \hat{x} + \Phi(\hat{x}) + \varphi(\hat{x}) + g(\hat{x})u \quad (7)$$

where

$$\Lambda = \left[\begin{array}{cc|cc|cc} 0 & 1 & 0 & 0 & 0 & 0 \\ 0 & 0 & 0 & 0 & 0 & 0 \\ \hline 0 & 0 & 0 & 0 & 0 & 0 \\ \hline 0 & 0 & 0 & 0 & 0 & 1 \\ 0 & 0 & 0 & 0 & 0 & 0 \end{array} \right] \quad (8)$$

$$\Phi(\hat{x}) = \begin{bmatrix} 0 \\ -\frac{b}{m}\dot{\hat{y}} + \frac{A_p \hat{P}_L}{m} \\ \hline -\frac{2\beta A_p}{V_0}\dot{\hat{y}} + \frac{2\beta k_q \hat{v}_e \sqrt{P_s - |\hat{P}_L|}}{V_0} \\ \hline 0 \\ -\omega_{nv}^2 \hat{v}_e - 2\epsilon_v \omega_{nv} \dot{\hat{v}}_e \end{bmatrix} \quad (9)$$

$$\varphi(x(t)) = \varphi(x(t), t) \Big|_{\eta(t)=[0, 0, 0]^T} \quad (10)$$

Therefore, the derivative of the observer state $\hat{x}_j^{\{i\}}(t)$, $\forall i \in [1, 2, 3]$, $\forall j = 0, \dots, r_i - 1$, being r_i the relative degree of the i -th output, can be estimated in finite time from the measured outputs $z_i = h_i(x)$ by means of a high-order sliding-mode differentiator [38]:

$$\begin{aligned} v_{-1}^{\{i\}} &= z_i \\ \dot{\sigma}_j^{\{i\}} &= v_j^{\{i\}} \\ e_j^{\{i\}} &= \sigma_j^{\{i\}} - v_{j-1}^{\{i\}} \\ v_j^{\{i\}} &= -\nu_j^{\{i\}} M_{\{i\}}^{1/(r_i-j+1)} [e_j^{\{i\}}]^{(r_i-j)/(r_i-j+1)} + \sigma_{j+1}^{\{i\}} \\ e_{r_i}^{\{i\}} &= \sigma_{r_i}^{\{i\}} - v_{r_i-1}^{\{i\}} \\ \dot{\sigma}_{r_i}^{\{i\}} &= -\nu_{r_i}^{\{i\}} M_{\{i\}} [e_{r_i}^{\{i\}}]^0 \end{aligned} \quad (11)$$

with $j \in 0, \dots, r_i - 1$, and where the following notation is adopted

$$[x]^y = |x|^y \text{sign}(x)$$

Note that $[x]^0 = \text{sign}(x)$. According to [38],

$$\nu_j^{\{1,3\}} = [3, 1.5, 1.1], \quad \nu_j^{\{2\}} = [1.5, 1.1] \quad (12)$$

where the gain $M_{\{i\}}$ should be selected to properly tune the observer convergence rate. In the following, two adaptive techniques for the selection of $M_{\{i\}}$ will be discussed, and the results will be compared with manually tuned gains. From the observer design, it follows that

$$\dot{\hat{x}}_j^{\{i\}} = \sigma_j^{\{i\}}, \quad j \in 0, \dots, r_i - 1, \quad \dot{\hat{x}}_{r_i}^{\{i\}} = \sigma_{r_i}^{\{i\}}$$

Since the finite-time exact estimates of \hat{x} are available via the higher-order sliding-mode differentiator (11), an estimation of the disturbance input vector can be provided by means of

$$\hat{\varphi}(\hat{x}, t) = \sigma - \Lambda \hat{x} - \Phi(\hat{x}) - g(\hat{x})u \quad (13)$$

where, from (11), $\sigma = [\sigma_1^{\{1\}} \sigma_2^{\{1\}} \sigma_1^{\{2\}} \sigma_1^{\{3\}} \sigma_2^{\{3\}}]^T$ is the observer augmented state, i.e. the estimated system state derivative.

The model parameters are determined by means of an identification procedure [39], and they are reported in Tab. 1.

3.1. Gain Adaptation

The only parameters to be tuned in the HSMO are the gains $M_{\{i\}}$. This parameter influences the convergence rate of the observer in a way that will be clarified later. Apart from manual tuning, a technique reported in literature [34, 35] is based on increasing these gains at a fixed rate whenever the error is different from zero in the ideal case, or larger than a proper threshold considering measurement disturbances. Therefore, in case of automatic gain tuning, the gains are not constant anymore, but their time derivative can be expressed as:

$$\dot{M}_{\{i\}} = \begin{cases} k_{\{i\}}, & |e_0^{\{i\}}| > \delta_{\{i\}} \\ 0, & |e_0^{\{i\}}| \leq \delta_{\{i\}} \end{cases} \quad (14)$$

where $\delta_{\{i\}}$ are the error thresholds. For the stability analysis of such a kind of AHSMO, the reader may refer to [34].

In the novel technique here proposed, called A+HSMO to distinguish it from the previous one, the gain adaptation rate is not constant when the error exceeds its threshold, but it is proportional to the absolute error itself, i.e.

$$\dot{M}_{\{i\}} = \begin{cases} k_{a\{i\}} |e_0^{\{i\}}|, & |e_0^{\{i\}}| > \delta_{\{i\}} \\ 0, & |e_0^{\{i\}}| \leq \delta_{\{i\}} \end{cases} \quad (15)$$

Table 1: Nominal parameters of the hydraulic actuator.

Description	Symbol	Unit	Value
Piston mass	m	kg	440
Piston area	A_p	m ²	0.01
Centered camera volume	V_0	m ³	0.004
Bulk modulus	β	Pa	1e9
Nominal valve gain	k_q	m ³ /(s V Pa ^{1/2})	6e-7
Input gain	k_e		0.49
Valve natural frequency	ω_{nv}	s ⁻¹	152
Valve damping coeff.	ϵ_v		0.92
Supply pressure	P_s	Pa	1e7

The advantages provided by the proposed gain-adaptation law are: 1) a faster convergence in case of initial large estimation errors, e.g. in case of large uncertainties on the initial state, since a direct relation between the error magnitude and the gain variation rate is exploited; 2) an additional degree of freedom provided by the coefficient $k_{a\{i\}}$ to independently tune the convergence rate of the observer during the initial transient, thanks to the fact that $k_{a\{i\}}$ linearly multiplies the absolute error value; 3) a limited gain variation in case of sporadic violation of the estimation error threshold after the initial transient, because after the initial transient the estimation error magnitude is very likely quite small. These properties will be validated during the experimental tests.

It is worth noting that it is certainly not a new idea to tune the observer parameters based on the estimation errors as in eq. (15). However, the proposed technique is not actually reported in existing literature related to HSMO.

A key issue on threshold-based adaptation methods such as eq. (14) and (15) is how to choose the thresholds $\delta_{\{i\}}$. While a large threshold value may result in large estimation errors due to the smaller value the observer gain will achieve, a small threshold may generate continuously increasing gains due to measurement noise. Therefore, on the basis of an experimental evaluation of the state observation error, the threshold values should be selected large enough to avoid the observer gain, after the initial transient, to be affected by the measurement noises. Generally speaking, after an experimental evaluation of the measurement noises, the values of the threshold $\delta_{\{i\}}$ should be selected just larger than the measurement noise level on the corresponding i -th output in order to achieve a steady state value of the observer gains.

3.2. Stability analysis

For the stability analysis of the proposed A+HSMO, we have first to highlight the fact that the observer of the system at hand can be seen as the composition of two differentiator types:

- Two second-order differentiators for the piston rod and the valve dynamics (the first and the third equation in (1) respectively);
- A first-order differentiator for the hydraulic circuit dynamics (the second equation in (1)).

Therefore, it is possible to split the stability analysis of the proposed AHSMO into the analysis of a first-order and of a second-order differentiator with the proposed gain adaptation law. For this reason and for the sake of brevity, the index $\{i\}$ is dropped in the following.

As a general observation, according to [40], it is possible to show how the Lyapunov functions for the designed sliding-mode differentiators scale with the value of the gain M , the interested reader

may refer to [41] for the details. Therefore, given a Lyapunov function for a specific value of the observer gain M , it is possible to obtain a Lyapunov function for any value of M by a suitable scaling of the parameters. For this reason, the value of the gain used to define the Lyapunov function for the non-adaptive part is omitted in the following.

3.2.1. Stability of the adaptive-gain second-order differentiator

The following Lyapunov function is adopted

$$V(\epsilon, M) = V_0(\epsilon) + \frac{1}{4}(M - M^*)^4 \quad (16)$$

where

$$\epsilon = [[e_0]^{2/3} \quad e_1 \quad [e_2]^2]^T$$

is the observer state vector adopted for stability analysis, M^* represents a suitable upper bound to the gain values, $V_0(\epsilon)$ is the Lyapunov function for the non-adaptive differentiator as proposed in [40]:

$$V_0(\epsilon) = \epsilon^T \Gamma \epsilon, \quad \Gamma = \begin{bmatrix} \gamma_1 & -\frac{1}{2}\gamma_{12} & 0 \\ -\frac{1}{2}\gamma_{12} & \gamma_2 & -\frac{1}{2}\gamma_{23} \\ 0 & -\frac{1}{2}\gamma_{23} & \gamma_3 \end{bmatrix}$$

where Γ is a positive definite and radially unbounded symmetric matrix if and only if

$$\gamma_1 > 0, \quad \gamma_1\gamma_2 - \frac{1}{4}\gamma_{12}^2 > 0, \quad \left[\gamma_1\gamma_2 - \frac{1}{4}\gamma_{12}^2 > 0 \right] \gamma_3 - \frac{1}{4}\gamma_1\gamma_{23}^2 > 0$$

It is possible to show that, since the observer error in the non-adaptive case converges in finite time to the origin also in case of perturbations for any value of the gain $M \geq 1$ [40], the gain-adaptation law will reach the condition $\dot{M} = 0$ in finite time, i.e. as soon as $|e_0| \leq \delta$. Therefore, it is possible to assume that there exists a positive constant M^* such that $M(0) = 1$, $M < M^*$, $\forall t \geq 0$.

If $|e_0| \leq \delta$, it follows that $\dot{M} = 0$ and

$$V(\epsilon, M) = V_0(\epsilon) \quad (17)$$

With reference to the general definition of the HSMO eq. (11), it is possible to show that $\dot{V}_0(\epsilon)$ is negative definite if the following additional conditions are satisfied

$$\gamma_{12} > 0, \quad \gamma_{23} > 0, \quad \nu_{r_i} M > \eta(t) \quad \forall t$$

for some positive values of the gains ν_j , $j = 0, \dots, r_i$ as reported in (12), where $\eta(t)$ is the disturbance acting on the system and the dependance from the specific observer index $\{i\}$ is removed for

generality. For the interested reader, the complete demonstration about the negative definitiveness of $\dot{V}_0(\epsilon)$ is reported in [40].

If $|e_0| > \delta$, from (16) it follows that

$$\begin{aligned}\dot{V}(\epsilon, M) &= \dot{V}_0(\epsilon) + \dot{M}(M - M^*)^3 \\ &= \dot{V}_0(\epsilon) - k_a |e_0| |M - M^*|^3 < \dot{V}_0(\epsilon) - k_a \delta |M - M^*|^3\end{aligned}$$

It is important to recall that under the conditions given in Theorem 1 of [40], the following condition

$$\dot{V}_0(\epsilon) \leq -\vartheta V_0^{\frac{3}{4}}(\epsilon)$$

is satisfied for some positive constant ϑ . It is then possible to write

$$\dot{V}(\epsilon, M) \leq -\vartheta V_0^{\frac{3}{4}}(\epsilon) - k_a \delta |M - M^*|^3$$

By applying Jensen's inequality

$$|x| + |y| \geq (|x|^q + |y|^q)^{\frac{1}{q}}, \quad \forall q \geq 1$$

with $q = 4/3$, we obtain

$$\begin{aligned}\dot{V}(\epsilon, M) &\leq - \left[\vartheta^{\frac{4}{3}} V_0(\epsilon) + 4 (k_a \delta)^{\frac{4}{3}} \left(\frac{1}{4} |M - M^*|^4 \right) \right]^{\frac{3}{4}} \\ &\leq -\min \left(\vartheta, 4^{\frac{3}{4}} k_a \delta \right) V^{\frac{3}{4}}(\epsilon, M)\end{aligned}\tag{18}$$

It follows that, other than ensuring the observer stability, the proposed gain-adaptation law preserves also the finite-time convergence property of the second-order differentiator.

3.2.2. Stability of the adaptive-gain first-order differentiator

For the stability of the adaptive-gain first-order differentiator, the following candidate Lyapunov function is adopted

$$V(\epsilon, M) = V_0(\epsilon) + \frac{1}{2}(M - M^*)^2\tag{19}$$

where

$$\epsilon = [|e_0|^{1/2} \quad e_1]^T$$

is the observer state vector adopted for stability analysis, M^* represents a suitable upper bound to the gain value, $V_0(\epsilon)$ is the Lyapunov function for the non-adaptive differentiator as proposed in [42]

$$V_0(\epsilon) = \epsilon^T P \epsilon$$

where P is a suitably-selected positive definite symmetric matrix. The same considerations made in the case the second-order differentiator for the boundedness of the gain M hold also in this case.

If $|e_0| \leq \delta$, it follows that $\dot{M} = 0$ and

$$V(\epsilon, M) = V_0(\epsilon) \quad (20)$$

In particular, in the unperturbed case, i.e. $\eta(t) = 0$, the first-order differentiator dynamics can be rewritten as

$$\dot{\epsilon} = \frac{1}{|e_0|^{1/2}} A \epsilon, \quad A = \begin{bmatrix} -\frac{1}{2}\nu_0 M^{1/2} & \frac{1}{2} \\ -\nu_1 M & 0 \end{bmatrix}$$

the derivative of $V_0(\epsilon)$ can be written as

$$\dot{V}_0(\epsilon) = -\frac{1}{|e_0|^{1/2}} \epsilon^T Q \epsilon$$

where Q is a positive definite symmetric matrix, and P is related to Q by the algebraic Lyapunov equation

$$A^T P + P A = -Q \quad (21)$$

Since A is Hurwith if and only if $\nu_0 > 0$, $\nu_1 > 0$ and $M > 0$, a unique positive definite symmetric matrix P exists satisfying (21) for any positive definite symmetric matrix Q , so that $V_0(\epsilon)$ is a strict Lyapunov function for the first-order differentiator. In the perturbed case, i.e. $\eta(t) \neq 0$, it is possible to show that for $M > 1$ and with a suitable selection of positive values of the gains ν_0 , ν_1 as in (12) the estimation error converges to a suitable threshold in finite time. The interested reader may refer to [42] for further details on the selection of the first-order differentiator gains.

If $|e_0| > \delta$, from (16) it follows that

$$\begin{aligned} \dot{V}(\epsilon, M) &= \dot{V}_0(\epsilon) + \dot{M}(M - M^*) \\ &= \dot{V}_0(\epsilon) - k_a |e_0| |M - M^*| < \dot{V}_0(\epsilon) - k_a \delta |M - M^*| \end{aligned}$$

It is important to recall that under the conditions given in Theorem 1 of [42], the following condition

$$\dot{V}_0(\epsilon) \leq -\vartheta V_0^{\frac{1}{2}}(\epsilon)$$

is satisfied for some positive constant ϑ . Therefore, it is possible to write

$$\dot{V}(\epsilon, M) \leq -\vartheta V_0^{\frac{1}{2}}(\epsilon) - k_a \delta |M - M^*|$$

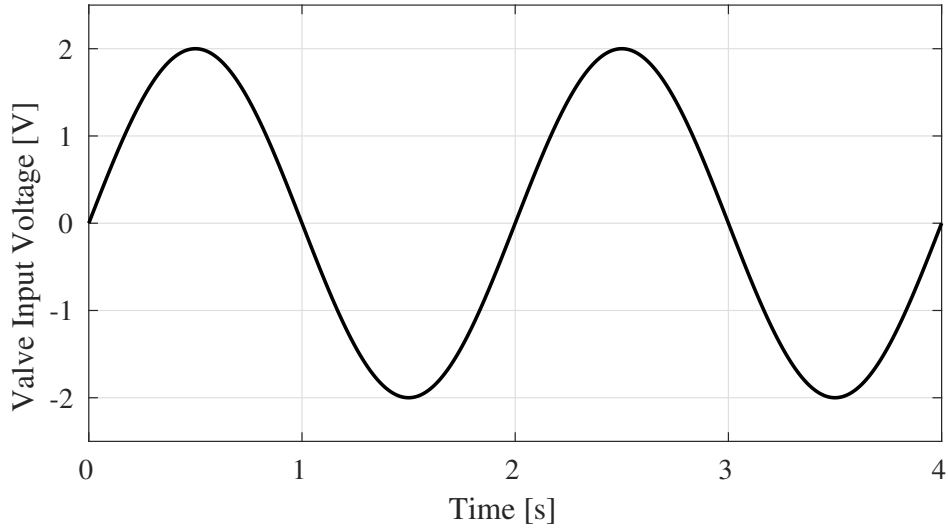


Figure 3: Valve input voltage adopted for all the tests.

By applying Jensen's inequality with $q = 2$, we obtain

$$\begin{aligned} \dot{V}(\epsilon, M) &\leq - \left[\vartheta^2 V_0(\epsilon) + 2 (k_a \delta)^2 \left(\frac{1}{2} |M - M^*|^2 \right) \right]^{\frac{1}{2}} \\ &\leq -\min \left(\vartheta, \sqrt{2} k_a \delta \right) V^{\frac{1}{2}}(\epsilon, M) \end{aligned} \quad (22)$$

It follows that, other than ensuring the observer stability, the proposed gain-adaptation law preserves also the finite-time convergence property of the first-order differentiator.

4. Experimental Results

Experimental tests are performed on the EHA test-bed to verify the effectiveness of the proposed approach for the HSMO gain adaptation. To evaluate the sensitivity of the designed state observers to different working conditions, two different experiments are performed: 1) without any load applied to the sliding table, as shown in left picture of Fig. 1; 2) with an Isolator Under Test (IUT) connected to the sliding table, as shown in right picture of Fig. 1.

In all the experimental tests, the input signal is the one reported in Fig. 3, and the HSMO is designed on the basis of the nominal system parameters reported in Tab. 1. Moreover, the manually-selected HSMO gains adopted for comparison are the same adopted in [32] and they are reported in Tab. 2.

Table 2: Manually-selected gains of the HSMO.

$M_{\{1\}}$	$M_{\{2\}}$	$M_{\{3\}}$
220	60000	1000

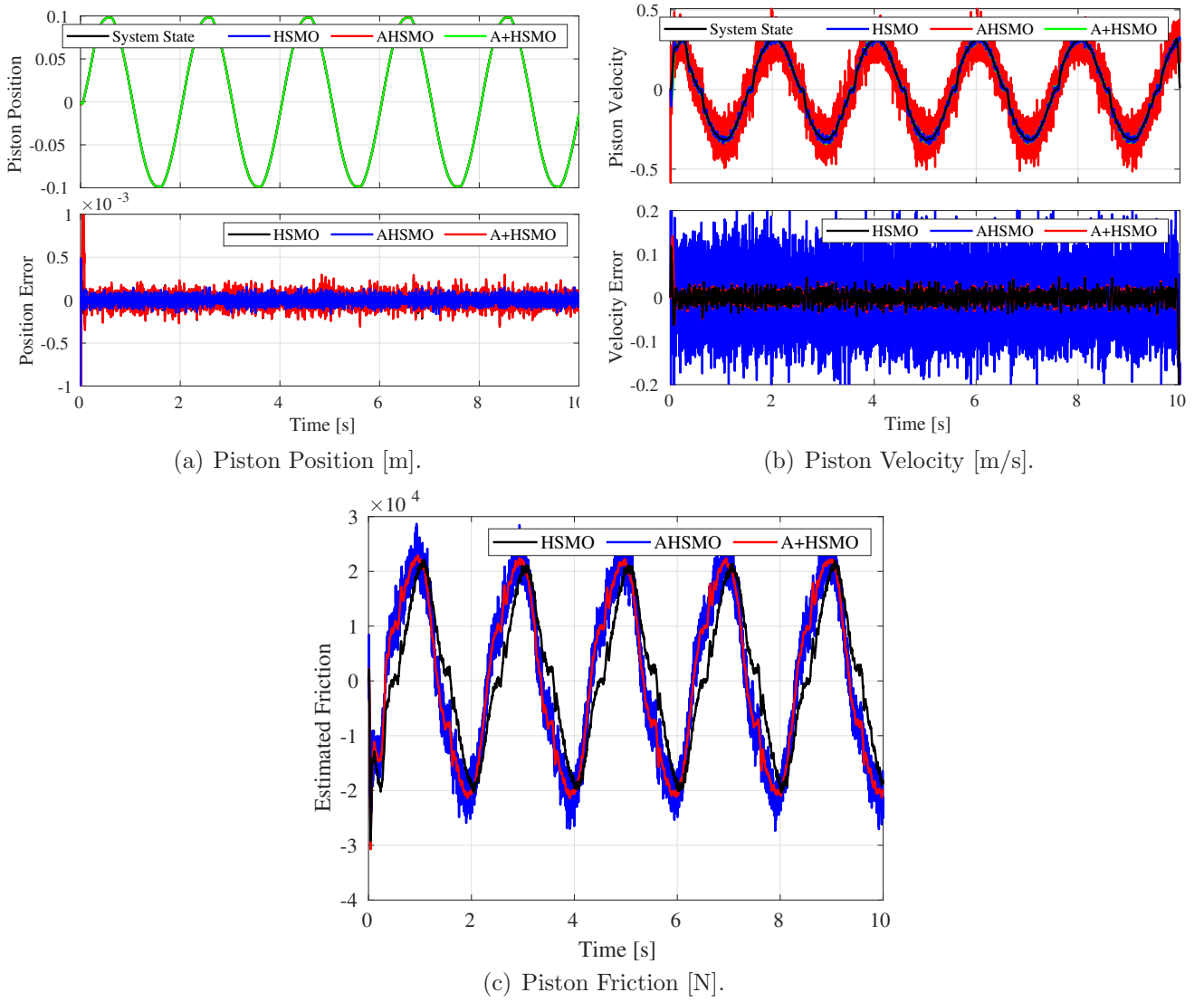


Figure 4: Piston position, velocity and friction during the experiment without IUT and estimation provided by the HSMO.

The experimental setup is equipped with sensors providing measurements of the piston position, pressure and valve spool position. However, no information is available from the valve manufacturer about the relation between the valve output position signal and the effective valve spool position. Therefore, the valve spool position and velocity will be expressed in volts and volts/seconds respectively to reflect the output position signal provided by the valve itself. For the comparison with the piston and spool velocities estimated by the observers, these data are reconstructed from the respective position information through digital filtering.

In the following, the experimental results will be reported in the aforementioned working conditions. After, those results will be discussed to draw some conclusion about the proposed gain-adaptation strategy.

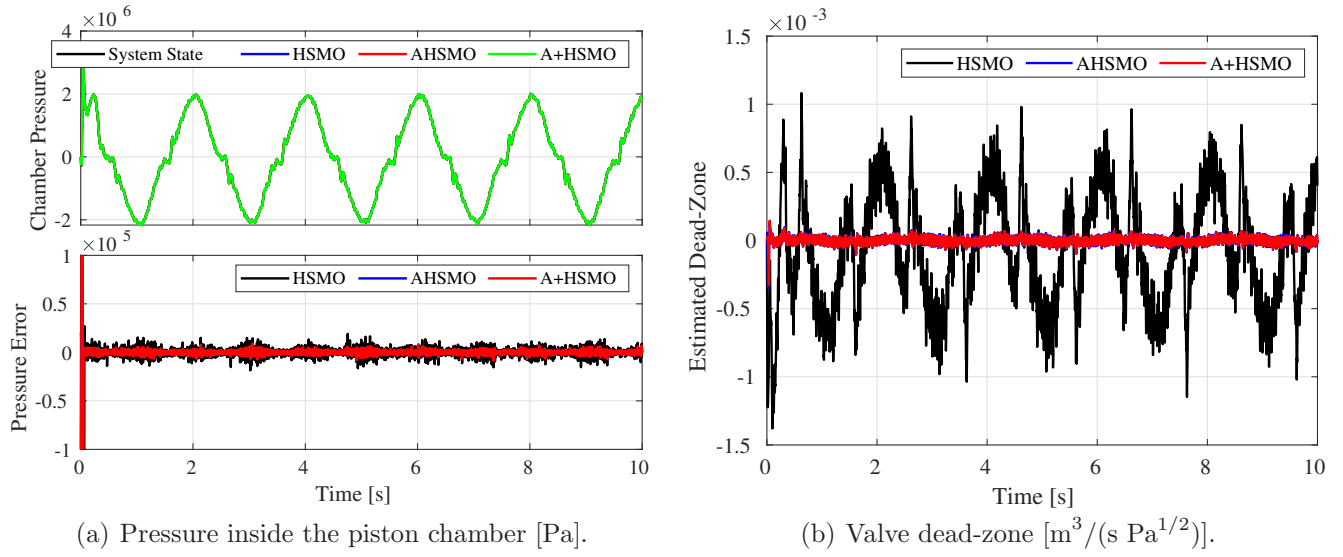


Figure 5: Pressure inside the piston chamber during the experiment without IUT and estimation provided by the HSMO.

4.1. Experimental results without piston load

The results of the experimental test in case of no EHA load are shown in Fig. 4, 5 and 6. The effective system state is compared with respect to the state estimated by the HSMO, AHSMO and A+HSMO. Moreover, the estimation error is also reported to ease the comparison. As previously mentioned, the designed observer provides also an estimation of the disturbances acting on the system. Therefore, those estimations are shown together with the state information. In particular, Fig. 4 reports the piston position (Fig. 4(a)), velocity (Fig. 4(b)) and the estimated friction (Fig. 4(c)). Figure 5 reports the pressure in the piston chamber (Fig. 5(a)) and the effect of the valve dead-zone (Fig. 5(b)). Finally, Fig. 6 reports the valve data, such as the valve spool position (Fig. 6(a)), velocity (6(b)) and estimated input bias (Fig. 6(c)).

To simplify the analysis of these results, the performance of the three observers in terms RMS value of the state estimation errors during the experimental tests without load applied to the EHA are reported in Tab. 4. The comparison of the gains of the AHSMO and the A+HSMO are reported respectively in Fig. 7(a) and 7(b).

Table 3: Parameter of the AHSMO and the A+HSMO.

index	$\{1\}$	$\{2\}$	$\{3\}$
$\delta_{\{i\}}$	3e-4	4000	0.4
$k_{\{i\}}$	1	1e6	1
$k_{a\{i\}}$	1	1	1

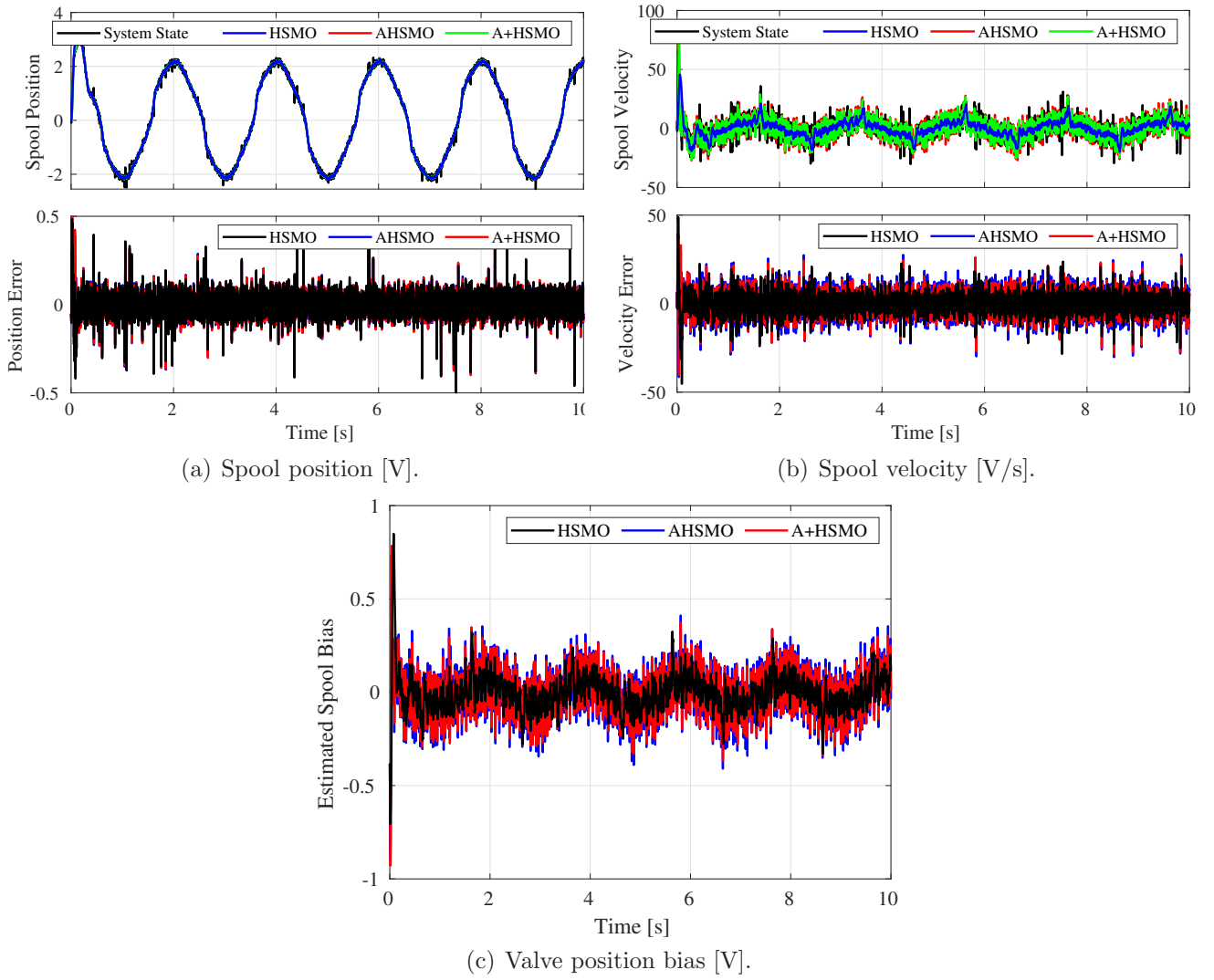


Figure 6: Valve position, velocity and input bias during the experiment without IUT and estimation provided by the HSMO.

4.2. Experimental results with nonlinear piston load

The results of the experimental test in case the IUT is attached to the piston are shown in Fig. 8, 9 and 10. In particular, Fig. 8 reports the piston position (Fig. 8(a)), velocity (Fig. 8(b)) and the estimated friction (Fig. 8(c)). Note that, with respect to the previous experiment, the piston load is significantly higher.

Figure 9 reports the pressure in the piston chamber (Fig. 9(a)) and the effect of the valve dead-zone (Fig. 9(b)).

Finally, Fig. 10 reports the valve position (Fig. 10(a)), velocity (10(b)) and estimated input bias (Fig. 10(c)).

As in the previous case, the performance of the three observers in terms RMS value of the state estimation errors during the experimental tests with IUT attached to the EHA are reported in

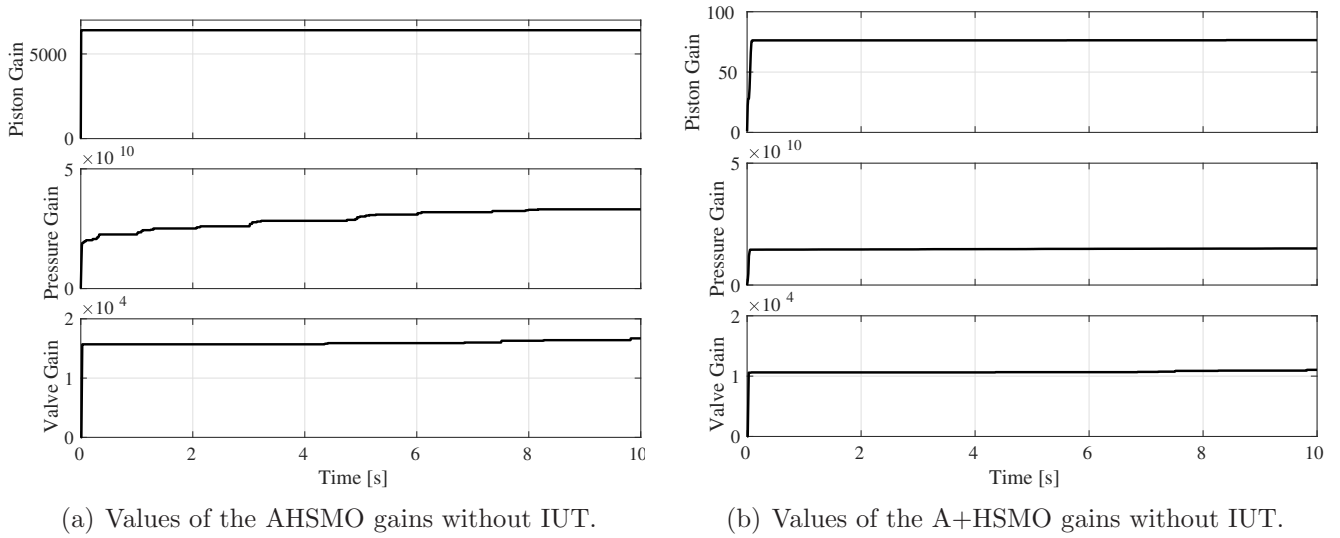


Figure 7: Comparison of the observer gains during the experiment without the IUT.

Tab. 5. The comparison of the gains of the AHSMO and the A+HSMO are reported respectively in Fig. 11(a) and 11(b).

4.3. Discussion of the Results

From all these results, and in particular looking to Tab. 4 and 5, is it possible to conclude that, while the AHSMO shows slightly better performance in case of the y estimation, it behaves worst than the other observers in all the other cases. On the other side, the A+HSMO performance is similar to the manually-tuned HSMO for all the state components but for the chamber pressure P_L , in which the A+HSMO RMS error is about one third of the HSMO one in case of no load and three to four times smaller in case of IUT attached to the piston. By directly comparing the AHSMO and the A+HSMO, it is possible to state that the latter shows overall better performance, in particular in the case of large signals such as P_L . It is also worth noticing that looking at Fig. 5(b) and 9(b), the larger value of the observer gain achieved by both the AHSMO and the A+HSMO generates a significantly different estimation of the valve dead-zone.

Another interesting consideration is the comparison of the gains of the AHSMO and the A+HSMO. From the plots reported in Fig. 7 for the case of no EHA load and in Fig. 11 in case of the IUT attached to the EHA, it is possible to see that, with respect to the AHSMO, the A+HSMO

Table 4: RMS value of the state estimation errors obtained during the experiment without IUT.

Experiment	y	\dot{y}	P_L	v_e	\dot{v}_e
HSMO	1.73e-7	0.63e-4	9.07	1.46e-4	1.17e-2
AHSMO	1.00e-7	1.92e-4	1.98	1.43e-4	1.82e-2
A+HSMO	2.02e-7	0.61e-4	3.37	1.45e-4	1.52e-2

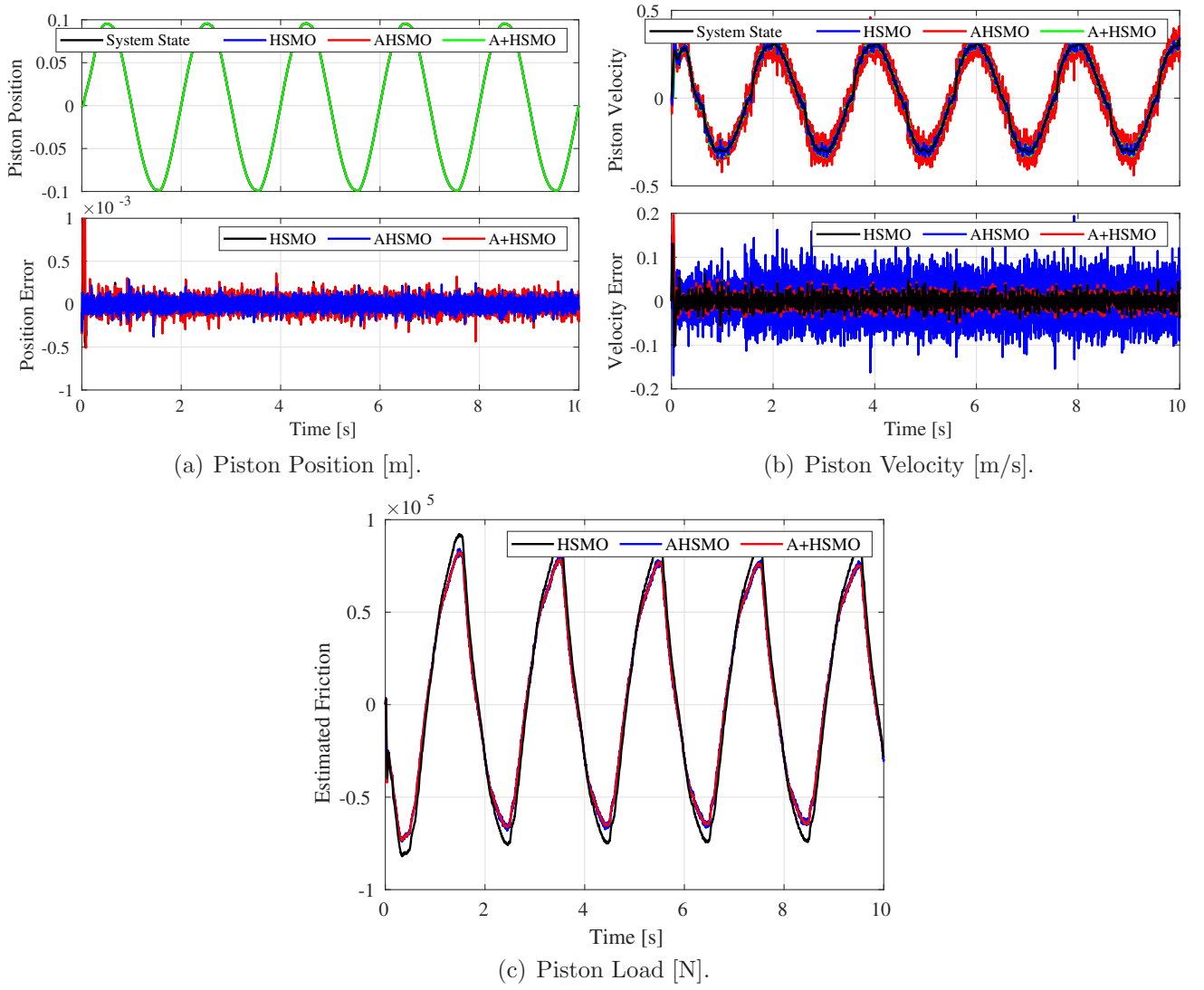


Figure 8: Piston position, velocity and friction during the experiment with IUT and estimation provided by the HSMO.

gains present a fast initial convergence followed by a limited variation. Moreover, the value of the A+HSMO gains are in general smaller than the AHSMO ones and that, after the initial transient, the A+HSMO gains reach a stable value, while the AHSMO gains continue to change along the experiment. This fact confirms the motivations at the basis of the A+HSMO design.

5. Conclusions

In this paper, the evaluation of a HSMO-based robust observation methods with adaptive gain selection applied to a hydraulic actuation system is reported, in case of noisy measurements, uncertain disturbances and unknown load.

A novel strategy for gain adaptation in HSMO, called A+HSMO, is defined and its stability analysis is provided, showing that it preserves all the properties of finite time convergence of the

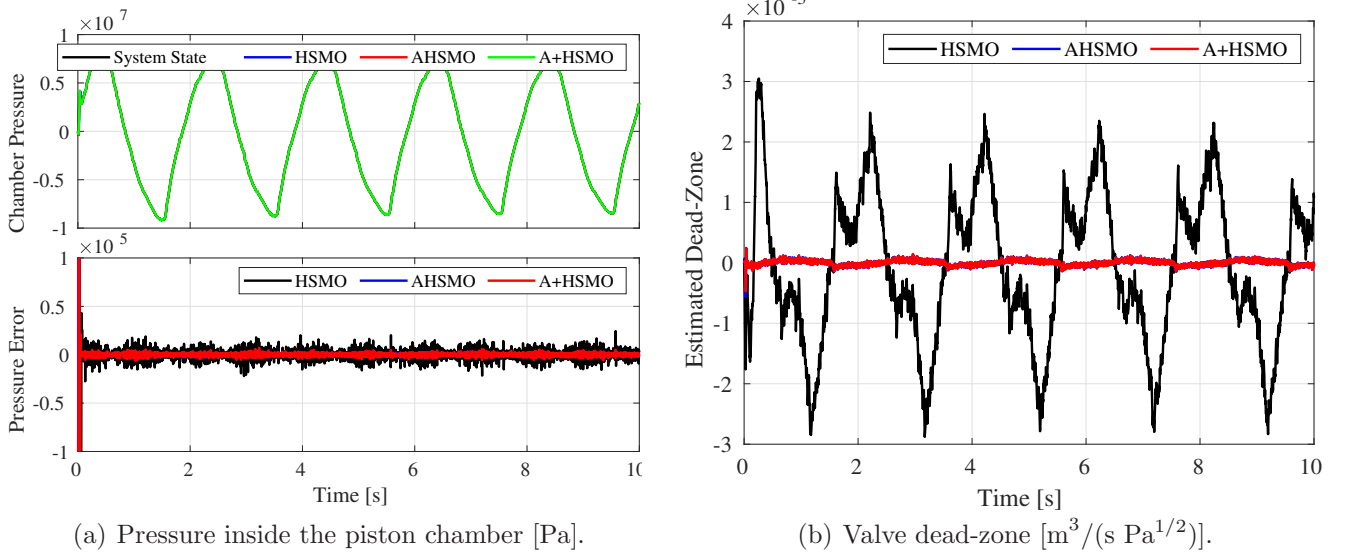


Figure 9: Pressure inside the piston chamber during the experiment with IUT and estimation provided by the HSMO.

state estimation error of its fixed-gain counterpart.

To validate the A+HSMO, experimental tests are performed both in case of no load attached to the hydraulic actuator and in case an unknown non-linear visco-elastic load is attached to the system. The A+HSMO shows the ability to provide a reliable estimation of the system state in all the test conditions. Moreover, the A+HSMO is compared with the case of manually tuned (fixed) gains and with a conventional gain adaptation strategy from the literature. The A+HSMO shows results comparable to the manually-tuned HSMO apart from the estimation of the chamber pressure that is significantly better for the A+HSMO. Moreover, the A+HSMO results to have better performance in almost all the cases with respect to the AHSMO, also from the point of view of the gains evolution.

References

- [1] S. Tafazoli, C. W. de Silva, P. D. Lawrence, Tracking control of an electrohydraulic manipulator in the presence of friction, IEEE Tran. on Control Systems Technology 6 (3) (1998) 401–411.

Table 5: RMS value of the state estimation errors obtained during the experiment with IUT.

Experiment	y	\dot{y}	P_L	v_e	\dot{v}_e
HSMO	2.00e-7	0.45e-4	1.15e1	1.49e-4	1.23e-2
AHSMO	1.40e-7	1.19e-4	0.19e1	1.55e-4	2.98e-2
A+HSMO	2.22e-7	0.47e-4	0.24e1	1.55e-4	3.06e-2

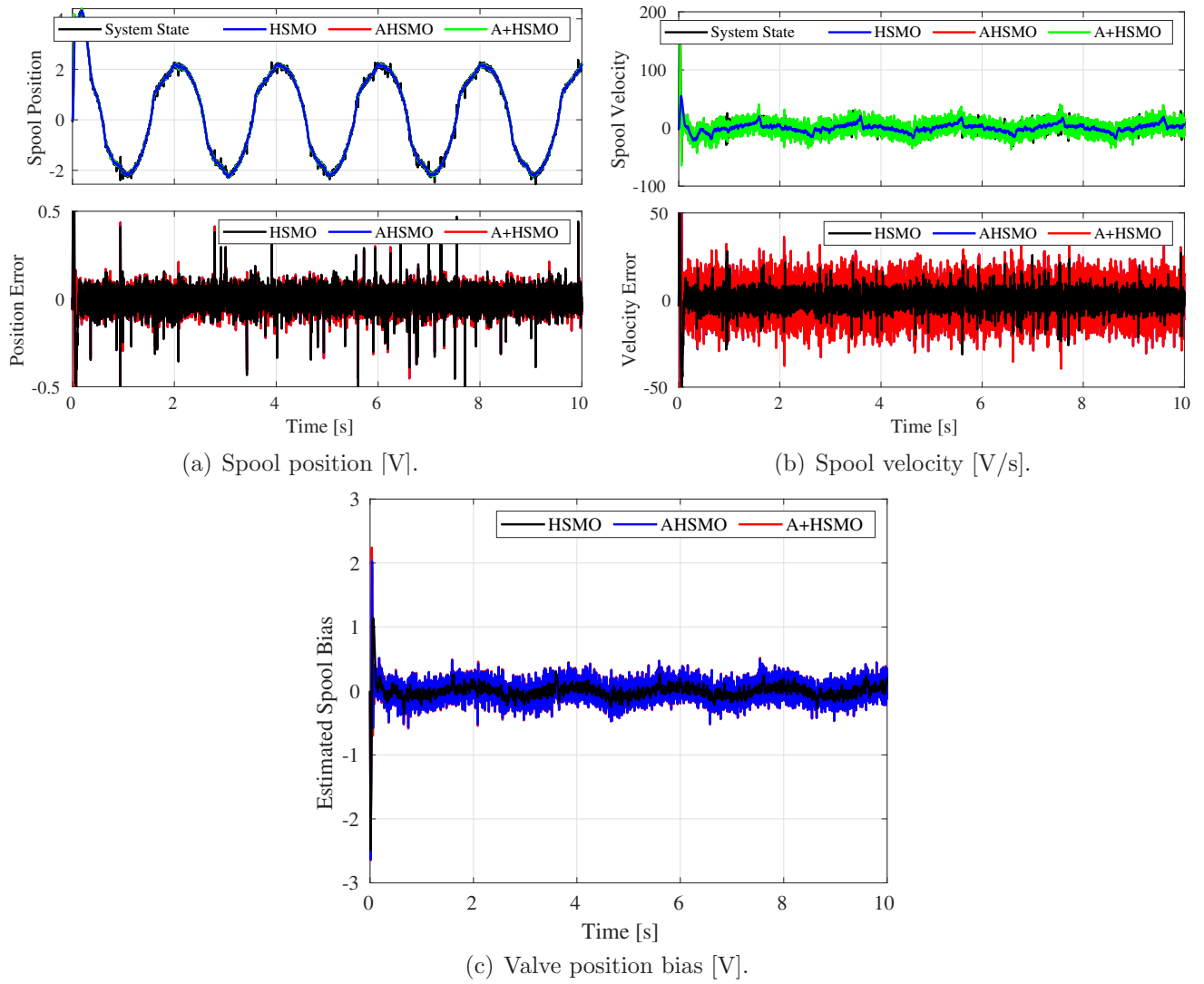


Figure 10: Valve position, velocity and input bias during the experiment with IUT and estimation provided by the HSMO.

- [2] A. Alleyne, Nonlinear force control of an electro-hydraulic actuator, in: Proc. of the Japan/USA Symposium on Flexible Automation, Vol. 1, 1996, pp. 193–200.
- [3] A. Alleyne, J. K. Hedrick, Nonlinear adaptive control of active suspensions, IEEE Tran. on Control Systems Technology 3 (1) (1995) 94–101.
- [4] X.-b. Fu, B. Liu, Y.-c. Zhang, L.-n. Lian, Fault diagnosis of hydraulic system in large forging hydraulic press, Measurement 49 (2014) 390–396.
- [5] A. Maddahi, W. Kinsner, N. Sepehri, Internal leakage detection in electrohydrostatic actuators using multiscale analysis of experimental data, IEEE Transactions on Instrumentation and Measurement 65 (12) (2016) 2734–2747.

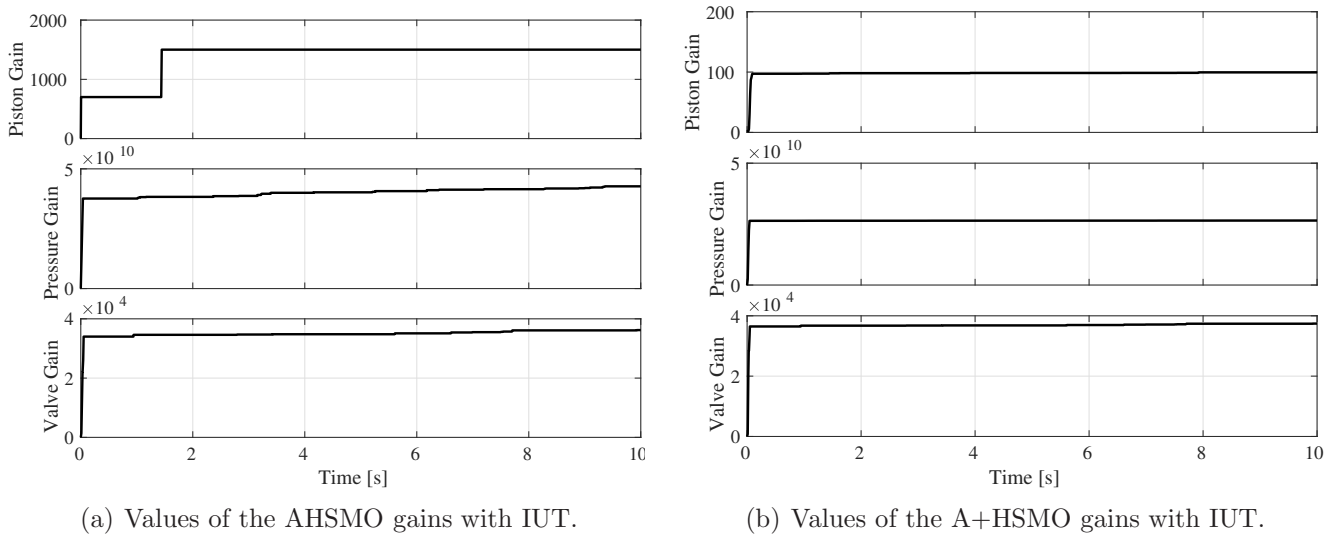


Figure 11: Comparison of the observer gains during the experiment with IUT.

- [6] H.-Z. Tan, N. Sepehri, Parametric fault diagnosis for electrohydraulic cylinder drive units, *IEEE Transactions on Industrial Electronics* 49 (1) (2002) 96–106.
- [7] C. C. DeBoer, B. Yao, Velocity control of hydraulic cylinders with only pressure feedback, in: *ASME International Mechanical Engineers Congress and Exposition*, 2001.
- [8] T. Virvalo, Nonlinear model of analog valve, in: *Proc. of the 5th Scandinavian International Conference of Fluid Power*, Vol. 3, 1997, pp. 199–213.
- [9] D. Yu, Fault diagnosis for a hydraulic drive system using a parameter-estimation method, *Control Engineering Practice* 5 (9) (1997) 1283–1291.
- [10] G. J. Preston, D. N. Shields, S. Daley, Application of a robust nonlinear fault detection observer to a hydraulic process, in: *Proc. of UKACC Intl. Conf. Control*, 1996, pp. 1484–1489.
- [11] H. Hammouri, P. Kabore, S. Othman, J. Biston, Failure diagnosis and nonlinear observer. application to a hydraulic process, *Journal of the Franklin Institute* 339 (4) (2002) 455–478.
- [12] L. An, N. Sepehri, Hydraulic actuator circuit fault detection using extended kalman filter, in: *Proceedings of the 2003 American Control Conference*, 2003., Vol. 5, 2003, pp. 4261–4266.
- [13] M. Khoshzaban, F. Sassani, P. D. Lawrence, Online state and parameter estimation of an electrohydraulic valve for intelligent monitoring, in: *Proc. of IEEE/ASME Int. Conf. on Advanced Intelligent Mechatronics*, 1997.

- [14] P. Halder, A novel approach for detection and diagnosis of process and sensor faults in electro-hydraulic actuators, *International Journal of Engineering Research and Development* 6 (7) (2013) 15–22.
- [15] M. Sepasi, F. Sassani, On-line fault diagnosis of hydraulic systems using unscented kalman filter, *International Journal of Control, Automation and Systems* 8 (1) (2010) 149–156.
- [16] J. Yao, W. Deng, Active disturbance rejection adaptive control of hydraulic servo systems, *IEEE Transactions on Industrial Electronics* 64 (10) (2017) 8023–8032.
- [17] J. Yao, Z. Jiao, D. Ma, Extended-state-observer-based output feedback nonlinear robust control of hydraulic systems with backstepping, *IEEE Transactions on Industrial Electronics* 61 (11) (2014) 6285–6293.
- [18] S. Strano, M. Terzo, Accurate state estimation for a hydraulic actuator via a SDRE nonlinear filter, *Mechanical Systems and Signal Processing* 75 (2016) 576–588.
- [19] R. Rajamani, J. K. Hedrick, Adaptive observers for active automotive suspensions: theory and experiment, *IEEE Transactions on Control Systems Technology* 3 (1) (1995) 86–93.
- [20] P. Garimella, B. Yao, Nonlinear adaptive robust observer design for a class of nonlinear systems, in: *Proc. of the American Control Conference*, Vol. 5, 2003, pp. 4391–4396.
- [21] P. Garimella, B. Yao, Nonlinear adaptive robust observer for velocity estimation of hydraulic cylinders using pressure measurement only, in: *ASME Int. Mechanical Engineering Congress and Exposition, Dynamic Systems and Control*, New Orleans, Louisiana, USA, 2002.
- [22] S. D. Nguyen, S.-B. Choi, Q. H. Nguyen, A new fuzzy-disturbance observer-enhanced sliding controller for vibration control of a train-car suspension with magneto-rheological dampers, *Mechanical Systems and Signal Processing* 105 (2018) 447 – 466.
- [23] Y. jie Wu, G. fei Li, Adaptive disturbance compensation finite control set optimal control for pmsm systems based on sliding mode extended state observer, *Mechanical Systems and Signal Processing* 98 (2018) 402–414.
- [24] Y. Hu, H. Wang, Robust tracking control for vehicle electronic throttle using adaptive dynamic sliding mode and extended state observer, *Mechanical Systems and Signal Processing* 135 (2020) 106375.

- [25] A. Mohanty, S. Gayaka, B. Yao, An adaptive robust observer for velocity estimation in an electro-hydraulic system, *International Journal of Adaptive Control and Signal Processing* 26 (12) (2012) 1076–1089.
- [26] A. Levant, Sliding order and sliding accuracy in sliding mode control, *International Journal of Control* 58 (6) (1993) 1247–1263.
- [27] L. Fridman, Y. Shtessel, C. Edwards, X.-G. Yan, Higher-order sliding-mode observer for state estimation and input reconstruction in nonlinear systems, *Int. Journal of Robust and Nonlinear Control* 18 (4-5) (2008) 399–412.
- [28] Y. Zhou, Y. Soh, J. Shen, High-gain observer with higher order sliding mode for state and unknown disturbance estimations, *International Journal of Robust and Nonlinear Control* 24 (15) (2014) 2136–2151.
- [29] F. Zhu, J. Yang, Fault detection and isolation design for uncertain nonlinear systems based on full-order, reduced-order and high-order high-gain sliding-mode observers, *International Journal of Control* 86 (10) (2013) 1800–1812.
- [30] H. Ros, J. Davila, L. Fridman, High-order sliding mode observers for nonlinear autonomous switched systems with unknown inputs, *Journal of the Franklin Institute* 349 (10) (2012) 2975–3002.
- [31] J. J. Rath, K. C. Veluvolu, M. Defoort, Y. C. Soh, Higher-order sliding mode observer for estimation of tyre friction in ground vehicles, *IET Control Theory Applications* 8 (6) (2014) 399–408.
- [32] G. Palli, S. Strano, M. Terzo, Sliding-mode observers for state and disturbance estimation in electro-hydraulic systems, *Control Engineering Practice* 74 (2018) 58–70.
- [33] J. Liu, Contributions to Adaptative Higher Order Sliding Mode Observers : Application to Fuel Cell an Power Converters, Theses, Université de Technologie de Belfort-Montbeliard (2014).
- [34] J. Liu, S. Laghrouche, M. Harmouche, M. Wack, Adaptive-gain second-order sliding mode observer design for switching power converters, *Control Engineering Practice* 30 (2014) 124–131.

- [35] C. Yang, T. Ma, Z. Che, L. Zhou, An adaptive-gain sliding mode observer for sensorless control of permanent magnet linear synchronous motors, *IEEE Access* 6 (2017) 3469–3478.
- [36] H. Merritt, *Hydraulic Control Systems*, Wiley, 1967.
- [37] L. Mrton, S. Fodor, N. Sepehri, A practical method for friction identification in hydraulic actuators, *Mechatronics* 21 (1) (2011) 350–356.
- [38] A. Levant, Higher-order sliding modes, differentiation and output-feedback control, *International Journal of Control* 76 (9-10) (2003) 924–941.
- [39] S. Strano, M. Terzo, A multi-purpose seismic test rig control via a sliding mode approach, *Structural Control and Health Monitoring* 21 (8) (2014) 1193–1207.
- [40] J. Moreno, Lyapunov function for Levant’s second order differentiator, in: *Proceedings of the IEEE Conference on Decision and Control*, 2012, pp. 6448–6453.
- [41] F. Ortiz-Ricardez, T. Snchez, J. Moreno, Smooth Lyapunov function and gain design for a second order differentiator, Vol. 54rd *IEEE Conference on Decision and Control*, CDC 2015, 2015, pp. 5402–5407.
- [42] J. Moreno, M. Osorio, Strict Lyapunov functions for the super-twisting algorithm, *IEEE Transactions on Automatic Control* 57 (4) (2012) 1035–1040.